# Damage Identification Scheme Based on Compressive Sensing

Ying Wang[1] and Hong Hao[2]

## Abstract

Civil infrastructures are critical to every nation, due to their substantial investment, long service period, and enormous negative impacts after failure. However, they inevitably deteriorate during their service lives. Therefore, methods capable of assessing conditions and identifying damages in a structure timely and accurately have drawn increasing attentions. Recently, compressive sensing (CS), a significant breakthrough in signal processing, has been proposed to capture and represent compressible signals at a rate significantly below the traditional Nyquist rate. Due to its sound theoretical background and notable influence, this methodology has been successfully applied in many research areas. In order to explore its application in structural damage identification, a new CS based damage identification scheme is proposed in this paper, by regarding damage identification problems as pattern classification problems. The time domain structural responses are transferred to the frequency domain as sparse representation, and then the numerical simulated data under various damage scenarios will be used to train a feature matrix as input information. This matrix can be used for damage identification through an optimization process. This will be one of the first few applications of this advanced technique to structural engineering areas. In order to demonstrate its effectiveness, numerical simulation results on a complex pipe soil interaction model are used to train the parameters and then to identify the simulated pipe degradation damage and free-spanning damage. To further demonstrate the method, vibration tests of a steel pipe laid on the ground are carried out. The measured acceleration time histories are used for damage identification. Both numerical and experimental verification results confirm that the proposed damage identification scheme will be a promising tool for structural health monitoring.

**Keywords**: Compressive sensing, Damage identification, Civil infrastructure, Pattern recognition, Sparse representation

[1]School of Engineering, Deakin University, 75 Pigdons Rd, Waurn Ponds, VIC 3216, Australia

[2]School of Civil and Resource Engineering, the University of Western Australia, 35 Stirling Hwy, Crawley, WA 6009, Australia

# Introduction

Civil infrastructures, such as dams, long-span bridges, pipelines and building structures, are highly important for every nation, because their construction and maintenance need substantial investment, and most of them are expected to serve for a relatively long period. Structural failures usually lead to disasters that may affect people, animals and the environment. However, during their service lives, many factors impair structural safety and integrity, including environmental loads (for example: earthquake, wind and flood), mechanical damages, structural aging (such as corrosion, deterioration, and fatigue effects) and some human factors. Therefore, deterioration of structural conditions is inevitable. In order to identify and assess various damages in a structure quickly and correctly, numerous research works have been conducted (Sohn et al. 2003). As presented in Kolakowski et al (2006), there are usually two approaches for structural damage identification, namely model-based method and signal-based method. The model-based method is a conceptually straightforward but practically difficult approach in which the parameters of an actual system model are used directly to represent physical quantities such as the structural stiffness and damping ratio. It strongly depends on the accuracy of the numerical model and usually leads to a very challenging ill-conditioned inverse problem. Alternatively, signal-based method has also received considerable attentions from the civil, aerospace, and mechanical engineering communities because they are particularly more effective for structures with complicated nonlinear behavior and the incomplete, incoherent, and noise-contaminated measurements of structural response (Adeli and Jiang, 2006). They are also more cost effective and suitable for online structural monitoring.

In general, the signal-based damage identification methods can be regarded as pattern recognition approaches. Numerous such approaches have been proposed. Sohn et al. (2001) presented a study on Structural Health Monitoring (SHM) using statistical pattern recognition techniques. Two pattern recognition techniques based on time series analysis are successfully applied to fiber optic strain gauge data obtained from a surface-effect fast patrol boat by distinguishing data sets from different structural conditions. Gul and Catbas (2009) employed experimental data coming from different test structures and damage cases to examine a statistical pattern recognition approach for SHM and discussed its advantages and drawbacks. With regard to wavelet-based methods, Kim and Melhem (2004) presented an informative literature review. The methods can be classified into three categories: 1) variation of wavelet coefficients, 2) local perturbation of wavelet coefficients in a space domain, and 3) reflected wave caused by local damage. Yang et al (2004) proposed a method based on empirical mode decomposition and Hilbert transform to extract the information of damage from measured data. The method was then applied to a benchmark problem established by ASCE

and the results demonstrated its effectiveness. Taha and Jucero (2005) have demonstrated a method to quantify evidence of damage levels in structures by means of the computations of fuzzy set theory. The proposed method uses Jeffery's non-informative priori in a Bayesian updating scheme to infer fuzzy health "or damage" patterns. The model has been shown to be capable of identifying damage accurately. Also, some researchers applied intelligent algorithms to structural damage detection. Hao and Xia (2002) proposed a method directly comparing the measured frequencies and mode shapes before and after damage to detect structural damage. A Genetic Algorithm (GA) with real number encoding is applied to minimize the objective functions. Experimental test results demonstrated that the method gives better damage detection results for the beam than the conventional optimization method. Bakhary et al (2007) presented a statistical artificial neural network (ANN) method that accounts for the inevitable finite element (FE) modelling error and measurement noise for structural condition identification. The accuracy of the approach was proved using Monte Carlo simulation. Chen and Zang (2009) presented an artificial immune pattern recognition approach for damage classification in structures. Although numerous methods have been proposed as reviewed above, there are still some fundamental challenges for damage identification, including sampling rate for sensing, the discerning between noise and damage, etc. Therefore, robust and reliable methods capable of detecting, locating and estimating damage quickly whilst being insensitive to changes in environmental and operating conditions have yet to be agreed upon.

Recently, Compressive Sensing (CS), a significant breakthrough in signal processing, has been developed to capture and represent compressible signals at a rate significantly below the Nyquist rate (Candes et al. 2006a, Donoho 2006, Eldar and Kutyiok 2012). This changes the traditional view that the sampling rate must be at least twice the maximum frequency of the signal. CS theory is initially used to recover certain signals from far fewer samples or measurements than traditional methods use. To make it possible, CS relies on two principles: sparsity, which pertains to the signals of interest, and incoherence, which pertains to the sensing modality. The main train of thought is to combine the data compression and sampling (Candes et al. 2006a, Donoho 2006). First, the signals are represented in the transform domain, where the signals become sparse. Second, a measurement matrix must allow the signal reconstruction. Third, the original signals can be reconstructed by using measurement values through an optimization process, i.e. basis pursuit. Nowadays, CS has been applied in many fields, including compressive imaging (Wakin et al. 2006, Duarte et al. 2008), medical imaging (Lu and Vaswani 2009), time-frequency analysis (Borgnat and Flandrin, 2008), and many others. However, there are only a few papers focusing on its application in SHM till now. Cortial et al (2007) may be the first authors who apply CS to SHM, for the development of a Dynamic Data Driven Applications System. The simulation results demonstrate the potential of CS

for locating structural damage. Gurbuz et al (2009) integrated CS with Ground Penetrating Radar, an important remote sensing tool in civil engineering. The results show that CS is robust to noise, random spatial sampling and introduces increased resolution. Bao et al (2010) applied CS to data compression for SHM system. The results show that the values of compression ratios achieved using CS are not high, since the vibration data are not naturally sparse in the chosen wavelet bases. Wang and Hao (2010) presented a concise introduction of CS theory and proposed several potential applications to structural engineering. By using the experimental measurement results, the study demonstrated that the reconstruction results by CS are very good, even if the vibration data are not mathematically sparse.

Currently, the terminology “compressed sensing” is more and more often used interchangeably with “sparse recovery” (Eldar and Kutyiok 2012). Thus, CS is more generally regarded as a mathematical tool capable of finding sparse solutions to under-determined or over-determined linear equations under certain conditions, than its initial concepts in signal compression and sampling. A successful application in pattern recognition field is proposed by Yang et al. (2007) and then improved in Wright et al. (2009). A robust face recognition algorithm is constructed from the perspective of sparse representation. Unlike the conventional CS applications that target on the sparse signal reconstruction via basis pursuit, Yang et al. (2007) defined the basis as the prior knowledge of the training database and transferred the face recognition problem into seeking the sparse coefficient/representation of the specific basis using CS as a mathematical tool.

This provides a new angle for damage identification by using the measured data directly. In this paper, a new damage identification paradigm based on sparse representation and CS techniques is proposed, shown in the Methodology section. Then, a simulated complex pipe-soil interaction model is used for validating the new scheme. At last, the experimental vibration time histories of the pipe-soil system are used to demonstrate the performances of the proposed method in damage detection of civil infrastructure. The results show that the proposed method is a promising tool for protection of civil infrastructure.

# Methodology

The mathematical background underlying CS is deep and beautiful, which can be found in existing references (Candes 2006, Eldar and Kutyiok 2012). This section discusses its application in structural damage identification using vibration time histories directly. While we will concentrate on the development of the damage identification scheme, some necessary concepts and relevant theories will be addressed first.

## *Theoretical background*

Experimental signals can be used directly for damage identification purposes. In SHM, these signals are usually vibration or wave propagation time histories. When expressed in an appropriate basis, they usually have concise representations. Mathematically speaking, we have a vector $\mathbf{f} \in \mathbf{R}^N$ (experimental signal), which can be expanded in an orthonormal decomposition basis (such as a Fourier basis or wavelet basis) $\Psi = [\psi_1 \psi_2 \cdots \psi_N]$ as follows:

$$\mathbf{f} = \Psi \mathbf{x} = \sum_{i=1}^{N} x_i \psi_i \tag{1}$$

$$x_i = \psi_i^T \mathbf{f} \tag{2}$$

where $x_i$ is the weighting coefficients of **f**, and $\bullet^T$ represents transposition (Eldar and Kutyiok 2012). The signal **f** is compressible if the representation (Eq. (1)) has just a few large coefficients and many small coefficients. The implication of sparsity is then clear: when a signal has a sparse expansion, one can discard the small coefficients without much perceptual loss. The sparsity can be quantified as follows. The signal **f** is *K*-sparse if it is a linear combination of only *K* basis vectors; that is, only *K* of the $x_i$ coefficients in Eq. (1) are nonzero and ($N - K$) are zero. The case of interest is when $K << N$.

In Wang and Hao (2010), the Fourier transform of vibration signal is selected as the orthonormal basis. The results demonstrated that the vibration or wave propagation signals are usually sparser in the frequency domain than in the time domain.

Now, we consider expressing the measurement (projection) about each signal **f** by the following functions:

$$y_k = \varphi_k^T \mathbf{f}, k = 1, ..., M \tag{3}$$

where $y_k$ is a measurement vector of **f**. Arrange the measurements $y_k$ in an $M \times 1$ vector **y** and the measurement vectors $\varphi_k^T$ as rows in an $M \times N$ projection matrix $\Phi$ ($M < N$). By combining Eqs (1) and (3), **y** can be written as

$$\mathbf{y} = \Phi \mathbf{f} = \Phi \Psi \mathbf{x} = \Theta \mathbf{x} \tag{4}$$

where $\Theta = \Phi\Psi$ is an $M \times N$ matrix. The measurement (projection) process is usually not adaptive,

meaning that $\Phi$ is fixed and independent of the signal **f**. The first basis $\Psi$ is used to represent the object **f** as in Eq. (1) and the second $\Phi$ is used for sensing **f** as in Eq. (3).

CS is originally developed for the reconstruction of the length-$N$ signal **f** from $M < N$ measurements (the vector **y**). Since $M < N$, this problem appears ill-conditioned. However, if **f** is $K$-sparse and the $K$ locations of the nonzero coefficients in **x** are known, then the problem can be solved provided $M \geq K$ (Eldar and Kutyiok 2012). A sufficient condition for a stable solution for both $K$-sparse and compressible signals has been proposed and referred to as the restricted isometry property (RIP) (Candes and Tao 2005). This property essentially requires that every set of columns with cardinality less than $K$ approximately behaves like an orthonormal system. An important result is that if the columns of the projection matrix $\Phi$ are approximately orthogonal, then the exact recovery phenomenon occurs (Candes 2006).

In order to solve the reconstruction problem, fewer unknown coefficients are desired. This condition is referred to as incoherence. The coherence $\mu$ measures the largest correlation between any two elements of $\Psi$ and $\Phi$ as:

$$\mu(\Phi, \Psi) = \sqrt{N} \cdot \max_{1 \leq k, i \leq N} \left| \langle \varphi_k, \psi_i \rangle \right| \tag{5}$$

It is demonstrated in Donoho and Huo (2001) that sufficiently small values of the incoherence between $\Psi$ and $\Phi$ guarantee the possibility of ideal atomic decomposition (Chen et al. 2001). The more incoherent, the fewer projection coefficients are needed (Candes 2006).

Both the RIP and incoherence conditions can be achieved with high probability by selecting $\Phi$ as a random matrix (Candes and Tao 2005). It should be admitted that there are many other matrices suitable as projection matrices. But for simplicity, normally distributed random matrix is adopted for $\Phi$ in this study.

## *Problem formulation based on sparse representation*

In this study, the damage identification problem is transformed to an equivalent pattern classification problem, following the idea proposed by Yang et al. (2007). An important assumption is that when a new signal associated with unknown damage pattern is given, we should find a close pattern from the given data. Thus, the damage pattern of the new signal will be classified to a pattern provided by the given data, which leads to damage classification.

We assume that there are totally $n$ signals with $m$ damage patterns used as training examples (time

domain structural dynamic responses), provided that the experimental conditions are the same. Then, $n_j$ vectors $\mathbf{v}_{j,1}, \mathbf{v}_{j,2}, ..., \mathbf{v}_{j,n_j}$ are the features of the training data associated with damage pattern $j$. In this study, the features are calculated by transforming the time domain training data to the frequency domain through Fast Fourier Transform (FFT).

For all the $n$ signals ($n = n_1 + \cdots + n_m$), the feature matrix (like a dictionary in information retrieval field) can be represented as:

$$\mathbf{A} = [\mathbf{v}_{1,1}, \mathbf{v}_{1,2}, ..., \mathbf{v}_{1,n_1}, \mathbf{v}_{2,1}, ..., \mathbf{v}_{m,n_m}] \tag{6}$$

The feature $\mathbf{v}$ of any new signal associated with damage $j$ can be assumed to be represented as a linear superposition of the training data associated with the same damage:

$$\mathbf{v} = \alpha_{j,1}\mathbf{v}_{j,1} + \alpha_{j,2}\mathbf{v}_{j,2} + \cdots + \alpha_{m,n_m}\mathbf{v}_{m,n_m} \tag{7}$$

where $\alpha_{j,l}, l = 1, ..., n_j$ are sparse representation scalars for identifying damage. Then, $\mathbf{v}$, the feature of the new signal with damage pattern $j$, can be represented in terms of all the signals in the training set as

$$\mathbf{v} = \mathbf{A}\mathbf{z} \tag{8}$$

where $\mathbf{z} = [0, ..., 0, ..., \alpha_{j,1}, \alpha_{j,2}, ..., \alpha_{j,n_j}, 0, ..., 0]^T$ is a coefficient vector whose entries are mostly zero except those associated with damage pattern $j$. Thus, $\mathbf{z}$ is mathematically sparse. Comparing Eq. (8) with Eq. (1), $\mathbf{A}$, $\mathbf{v}$ and $\mathbf{z}$ in Eq. (8) are essentially $\Psi$, $\mathbf{f}$ and $\mathbf{x}$ in Eq. (1), respectively. Here, we deliberately choose other symbols in order to emphasize that the meaning of $\mathbf{A}$ in the proposed method is the feature matrix, while $\Psi$ represents a decomposition basis matrix. The meaning of $\mathbf{v}$ and $\mathbf{z}$ are the feature of the new signal and the coefficient vector, respectively, while $\mathbf{f}$ and $\mathbf{x}$ indicate the signal in its original domain and transformed domain, respectively. The damage identification problem is thus transformed into the problem to find the optimum $\mathbf{z}$ associated with damage pattern $j$ for the new signal feature $\mathbf{v}$.

It should be noted that in this study, the new feature vector is expressed as linear superposition of the feature matrix $\mathbf{A}$, as shown in Eq. (7). This relationship has been demonstrated suitable for structural damage identification in Sections of numerical studies and experimental verifications. More complex relationships may perform better, while they will not be the contribution of this paper and will be investigated in the near future.

## Problem solution by using $l_1$ optimization

Traditionally, the solution of the formulated problem (Eq. (8)) is obtained by solving the following optimization problem (Candes et al. 2006a):

$$(P_1) \qquad \mathbf{z} = \arg\min \|\mathbf{z}\|_2 \quad \textbf{s.t.} \quad \mathbf{Az} = \mathbf{v} \tag{9}$$

where $\|\cdot\|_2$ is the $l_2$-norm of vector $\mathbf{z}$. However, the traditional $l_2$ minimization will almost never find a $K$-sparse solution, returning instead a nonsparse $\mathbf{z}$ with many nonzero elements (Baraniuk, 2007). Since we need to find the sparse solution for damage identification purposes, the direct use of Eq. (8) may not yield satisfactory results, as demonstrated by Yang et al (2007).

Recently, CS theory provides a solution by using $l_1$ optimization (Chen et al 2001), as shown in the following.

First, a random projection matrix $\Phi \in \mathbf{R}^{d \times m}$ can be applied to both sides of Eq. (8):

$$\tilde{\mathbf{v}} = \Phi\mathbf{v} = \Phi\mathbf{Az} = \tilde{\mathbf{A}}\mathbf{z} \tag{10}$$

where $\tilde{\mathbf{A}}$ can be compared to $\Theta$, and $\tilde{\mathbf{v}}$ can be compared to $\mathbf{y}$ in Eq. (4). In fact, by multiplying both sides of Eq. (8) by the random projection matrix $\Phi$, the damage classification problem (to find an optimal $\mathbf{z}$ in Eq. (10) based on $\tilde{\mathbf{A}}$ and $\tilde{\mathbf{v}}$) is finally transformed into a compressive sensing problem (to determine optimal $\mathbf{x}$ in Eq. (4) based on $\Phi$, $\Psi$ and $\mathbf{y}$ for reconstructing $\mathbf{f}$).

In Eqs. (8) and (10), the representation of $\mathbf{z}$ can be sparsely represented with respect to a dictionary of damage patterns if the number of damage patterns is reasonably large. Further, the selection of random projection matrix guarantees RIP and the incoherence. Therefore, the conditions of the current problem satisfy those of the CS problem.

Then, based on CS theory, the optimum $\mathbf{z}$ can be found by solving the following problem $P_2$:

$$(P_2) \qquad \mathbf{z} = \arg\min \|\mathbf{z}\|_1 \quad \textbf{s.t.} \quad \left\|\tilde{\mathbf{v}} - \tilde{\mathbf{A}}\mathbf{z}\right\|_2 \le \varepsilon \tag{11}$$

where $\varepsilon$ indicate the error tolerance and $\|\cdot\|_1$ is the $l_1$-norm.

It should be noted that there are many algorithms to solve $P_2$, while the widely applied $l^1$-MAGIC

optimization method (Candes and Romberg, 2005) is adopted. It should be also noted that theoretically $\varepsilon$ should be taken as zero. However, for computational efficiency, it is set as 0.001 in this study (default value in $l_1$-MAGIC).

Ideally, the nonzero entries in the estimated vector **z** will be associated with the columns in $\widetilde{\mathbf{A}}$ from a single damage pattern. In this case, we can easily assign the new signal **v** to that damage. However, due to such factors as noise, the nonzero entries may be associated with multiple damages. The classification method proposed by Yang et al (2007) is adopted in this paper. For each damage pattern $j$, define that $\delta_j(\mathrm{z})$ is a vector whose only nonzero entries are the entries in **z** that are associated with damage $j$, and whose entries associated with all other subjects are zero. Then,

$$\textbf{identity(z)} = \arg\min_j r_j(\mathbf{z}), \textit{where}\ r_j(\mathbf{z}) = \left\|\widetilde{\mathbf{v}} - \widetilde{\mathbf{A}}\delta_j(\mathbf{z})\right\|_2 \tag{12}$$

Here, identity of **z** represents the identified damage class.

## *Damage identification scheme*

Based on the above discussions, the damage identification algorithm can be proposed as follows (Yang et al. 2007):

Algorithm 1

1. **Input**: the feature matrix **A** for $m$ damage patterns based on training data, the feature vector **v** of a new signal, and an error tolerance $\varepsilon$

2. Generate $q$ random projection matrices $\Phi^1,\ldots,\Phi^q$.

**for all** $p$=1,…,$q$

3. Compute features $\widetilde{\mathbf{v}} = \Phi^p\mathbf{v}$ and $\widetilde{\mathbf{A}} = \Phi^p\mathbf{A}$, and normalize the results

4. Solve the convex optimization problem $(P_2)$ $\mathbf{z} = \arg\min\|\mathbf{z}\|_1$ **s.t.** $\left\|\widetilde{\mathbf{v}} - \widetilde{\mathbf{A}}\mathbf{z}\right\|_2 \le \varepsilon$ (Eq. (11))

5. Compute $r_j^p(\mathbf{z}) = \left\|\widetilde{\mathbf{v}} - \widetilde{\mathbf{A}}\delta_j(\mathbf{z})\right\|_2$, for $j = 1,\ldots,m$

**end for**

6. For each damage pattern $j$, $E(r_j) = \mathbf{mean}\{r_j^1, ..., r_j^q\}$

7. **Output**: $\mathbf{identity(z)} = \arg\min_j E(r_j)$.

Although $l_1$ optimization method should be stable when random matrix $\Phi$ is used, it may affect the results to a very high degree. Since the computed results are close to the optimal solutions with an approximately 60-80% possibility, multiple random matrices are generated and the averaged result is used in this paper. This will largely improve the computation results. In order to get the balance of performance and computation duration, $q$ is taken as 100 in this study.

Also, it should be noted that the performance of the proposed method depends on the selection of training data. Based on the above discussions, theoretically, the more features in the data training process, the better identification results. Since experimental data are always limited in practice, in order to fulfill this requirement, numerically simulated data will be used for training purposes in this paper. Although there are discrepancies between numerical and experimental results, the responses of a high-quality numerical model should indicate similar changes as those of the real structure due to damage. This will be demonstrated in section of experimental verifications.

In order to construct the feature matrix **A**, damage patterns need to be defined first. In practice, there are infinite possible damage patterns, while this study classifies the damage in three levels. In the first level, several damage types may exist in one structure. For example, a RC beam may have crack damage, debonding damage, and corrosion damage, etc, and combinations of these damages. The effects of different damage types on structural responses will be different. In the second level, for each damage type, damage location becomes another classification factor. In the third level, for a specific damage type and a determined damage location, damage severity can be regarded as the last classification factor. This arrangement is coincident with Rytter's damage identification hierarchy (Rytter 1993), where the first three levels for damage identification are damage detection, damage location and damage assessment, respectively.

Based on the above discussions, CS based damage identification scheme can be proposed as shown in the following. The Algorithm 1 will be used repeatedly in the following three steps. In the first step, $m_1$ damage types will be classified. In the second step, $m_2$ damage locations can be identified. In the last step, $m_3$ damage severities will be determined. By using the proposed method, damage information in different levels can be acquired orderly.

Algorithm 2: Damage identification scheme

**Input**: the feature matrix **A** based on all the training data, a feature vector **v** from a new signal

Step 1

a. **A** is classified as $m_1$ damage patterns based on **damage types**

b. Perform Algorithm 1

c. **Output**: the identified damage type for **v**

Step 2

a. **A** is classified as $m_2$ damage patterns based on **damage locations**

b. Perform Algorithm 1

c. **Output**: the identified damage location for **v**

Step 3

a. **A** is classified as $m_3$ damage patterns based on **damage severities**

b. Perform Algorithm 1

c. **Output**: the identified damage severity for **v**

# Numerical studies

In order to demonstrate the effectiveness of the proposed method, this paper will present two case studies on a complex pipe-soil model. In the first case, only pipe degradation damage is considered, while in the second one, both pipe damage and free-spanning damage are investigated. In each case, the training process is presented first. Then, the proposed method is applied to damage identification under noise free condition. At last, damage identification under different assumed noise levels is performed.

## *Numerical model*

In this study, vibration responses of a pipe-soil model in the impact hammer test will be simulated

with commercial software ANSYS. In Wang et al. (2010), an FE model for this system is described in detail, as shown in Figure 1. The steel pipe is model as a beam and the soil under the pipe is modeled as distributed springs. In this model, the pipe is divided into 16 parts and a total of 16 springs under each part are considered. The concrete blocks at two ends of the pipe are simulated as two rotational springs. Through experimental calibration (Wang et al., 2010), the geometrical and material properties of this system are obtained and summarized in Table 1.

Based on the calibrated FE model, the impact test is simulated in ANSYS and the vibration responses can be easily obtained. In this study, to demonstrate the effectiveness of the CS based method, only the response at one point is used, meaning that only one sensor is required for damage identification. In order to match the same condition as the experiments (section of experimental verification), the hitting point is located at 0.19**L* (*L* is the total length of the beam) and the sensing point is located at 1/8**L* (the second accelerometer detailed in section of experimental verification).

Two damage types are considered in this section, namely degradation of the pipe and free-spanning damage (loss of the soil support). For pipe damage, damage severity $\theta_p$ is defined as the pipe stiffness ratio after and before damage, and damage location $L_p$ is the number of pipe element. For free-spanning damage, damage severity $\theta_s$ is defined as the ratio of the stiffness of the soil support after and before damage, and damage location $L_s$ is the soil spring number.

In calculations, each time domain numerical simulation result under various conditions is transformed into the frequency domain through FFT first. Then, based on the damage patterns defined in subsection of damage identification scheme, the frequency domain results are classified to construct the feature matrix **A**.

## *Case 1: Pipe degradation damage*

In this case, only pipe degradation damage is considered. Therefore, only the last two steps in subsection of damage identification scheme will be performed, namely damage location and assessment. The pipe includes 16 segments, so $m_2$=16. In reality, the degradation damage will not be very high, so we only consider that the stiffness ratio varies from 0.5 (50% damage) to 0.9 (10% damage). The increment is taken as 0.1, and thus $m_3$=5. The damage assessment will thus be within the precision of 10%. Totally, there are 80 damage cases. Numerical simulations are performed for these cases as well as the intact structure case. Therefore, the training data include 81 structural responses, related to 80 damage cases and 1 intact case.

Damage identification can be realized in steps 2 and 3. In Step 2, 80 damage cases (**A**) are classified

316 into 16 categories. The cases in each category have the same damage location but different damage
317 severities. The classification results based on the proposed algorithm will lead to damage location.
318 In Step 3, there are two options, which are 1) the five damage cases with the identified damage
319 location are selected and then divided into five patterns based on their damage severities; 2) the total
320 80 damage cases are divided into five patterns with the same damage severity but different damage
321 locations. The comparison results will be given in the following. The classification results after this
322 step will identify damage severities.

323 **Damage identification under noise free condition**

324 This section focuses on damage identification under noise free condition. The simulated data with
325 randomly selected degradation damage ($L_p = 13; \theta_p = 0.54$) are used as the first example for
326 damage identification. The second example is $L_p = 4; \theta_p = 0.82$.

327 The classification results are summarized in Table 2. In each damage case, the proposed algorithm is
328 performed for three times. It can be seen that although random projection matrices are adopted in
329 this study, the classification results are stable. Specifically, the right damage location can be
330 accurately identified in Step 2. In Step 3, the closest damage severity result can be found by
331 choosing the first option. However, if we choose the second option by disregarding the information
332 that has been acquired in Step 2, the classification results become unstable. The results indicate the
333 importance of damage location information. Therefore, in the following, the first option is selected.

334 In order to find more accurate results, finer damage severity increment can be considered. In this
335 example, the increment is taken as 0.01 and the stiffness ratio varies from 0.50 to 0.99. Thus, $m_3$=50.
336 Since damage location has been determined, only 50 damage cases with known damage locations
337 but varying damage severities need be simulated. Based on these simulated results, the proposed
338 method can successfully identify the exact pipe degradation damage for above two cases,
339 specifically, $L_p = 13; \theta_p = 0.54$ and $L_p = 4; \theta_p = 0.82$. This demonstrates that finer damage
340 severity increments and/or more segments will give more damage patterns and higher precision
341 levels. In engineering practices, more training data can be simulated and thus more accurate results
342 can be obtained. However, the objective of this study is to demonstrate the effectiveness of the
343 proposed method. Therefore, in the following, the segments are still taken as 16 and the stiffness
344 ratio increment stays 0.1.

345 In fact, theoretically, with sufficient training data, the proposed method can achieve similar updating
346 results as the traditional FE model updating method, namely damage location and severity. The most

obvious advantage of the proposed method is that it only requires one measurement point. Under this condition, the traditional vibration based methods can only acquire part of the natural frequency information. In order to get high-quality damage identification results, the information of mode shapes are usually needed, which can only be achieved by using more measurement points.

The second advantage of the proposed method is the computational efficiency. The training data can be easily obtained from FE modeling and transformed to the frequency domain. The damage identification algorithm itself does not need to be changed. On the contrary, methods using ANN and other intelligent algorithms need be trained case by case. Also, the traditional FE model updating methods need to calculate the structural responses using FE models in each iteration, while the proposed method only needs computation of sparse matrices. These imply that the proposed method can save lots of computation time for damage identification.

The advantages of the proposed method indicate that it is more suitable for continuous online structural monitoring than the existing method as it is computationally more efficient and requires measurement at only one point.

**Damage identification under different noise levels**

In order to further demonstrate the effectiveness of the proposed method for practical application, it is used for damage identification using vibration data smeared with noise of different levels. The same two simulated damage cases are considered, specifically, $(L_p = 13; \theta_p = 0.54)$ and $(L_p = 4; \theta_p = 0.82)$. The numerically simulated vibration data are smeared with white noises. Three noise levels (in terms of the ratio of mean value of noise to signal) are considered, namely 1%, 5% and 10%. The normally distributed noises are added to the original signal.

The identified results are given in Table 3. As can be noted, the proposed algorithm correctly identifies the damage locations and very closely identifies the damage severity with the data smeared with noises of three levels. The results demonstrate that even under relatively high noise levels (10%) the proposed method is still robust and effective. The reason is that we set $q$ as 100, which minimizes the effects of random noises by averaging the results.

**Damage identification at multiple locations**

In the above two examples, the proposed method is used to identify only one damage in the structure. To further demonstrate the method, it is used for identification of multiple pipe degradation damages. Three cases are considered in this section. First, the simulated damages are

assumed at $L_p = 3$ with $\theta_p = 0.73$ and $L_p = 11$ with $\theta_p = 0.88$. Using the proposed scheme, the damage is exactly located at $L_p = 3$ and its severity is approximately estimated as $\theta_p = 0.7$. However, the second damage at $L_p = 11$ with $\theta_p = 0.88$ is not identified. In the second example, the simulated damages are assumed at $L_p = 4$ with $\theta_p = 0.93$ and $L_p = 12$ with $\theta_p = 0.68$. Using the proposed scheme, again only the severer damage is identified with the identification result of $L_p = 12$ and $\theta_p = 0.7$. In the third example, three simulated damages are assumed at $L_p = 3$ with $\theta_p = 0.68$, $L_p = 4$ with $\theta_p = 0.88$ and $L_p = 11$ with $\theta_p = 0.72$. Using the proposed scheme, again only the most severe damage at $L_p = 3$ is identified with the identified severity of $\theta_p = 0.6$. These three examples indicate that the proposed damage identification scheme can only find the most severe one among the damages, but failed to identify the less severe damages in the structure, Further, as can be noted in the above three examples, the identification results tend to overestimate the damage severity. Similar observations can be made if multi damages have the same damage severities. For example, assuming two damages at $L_p = 13; \theta_p = 0.82$ and $L_p = 4; \theta_p = 0.82$, using the above analysis, only one damage at $L_p = 3$ with the severity of $\theta_p = 0.8$ is identified.

In order to identify all the damages, multiple identification steps are proposed. Irrespective of the number of damages in a structure, use the above proposed approach to perform the first step analysis, which will lead to successful identification of the most severe damage in the structure. Then more numerical simulations of the structure with the identified damage in the structure will be carried out. In the second step numerical simulations, same approach as described above is used, except that the damaged element that has already been identified in the first step is excluded and the damage severity is assumed smaller than or equal to the one identified in the first step. For example, in the above first example, the identified damage in the first step is $L_p = 3$ with a severity of $\theta_p = 0.73$, then in the second step numerical simulations, only damages in 15 elements ($L_p = 1, 2, 4, 5 \ldots, 16$) excluding element 3, and damage severity of $\theta_p = 0.7, 0.8, 0.9$ will be simulated. 45 damage cases will be included into the training data in the second step. Using the data set from the second step numerical simulations and the same approach, the second damage is successfully located at $L_p = 11$ and its severity is estimated as $\theta_p = 0.9$. This approach can be repeated again to identify the next smaller damage in the structure in the next step analysis until there is no damage in the structure. The results demonstrate that the proposed multi-step damage identification method is robust to identify multiple damages in a structure.

## *Case 2: Multiple types of damage*

The second case will focus on identifying multiple types of damages on the pipe-soil system. Two damage types, namely damage on pipe and damage on soil spring supports, are considered in this study. In this case, damage identification is realized in three steps and $m_1$=2. There are 16 pipe segments and 16 soil springs as illustrated in Figure 1, so $m_2$=16 for both damage types. For the same reasons as stated in subsection of Case 1: Pipe degradation damage, the stiffness ratio for pipe degradation damage considered in numerical simulations are ranged from 0.5 to 0.9 and the increment is taken as 0.1. Thus, $m_3$=5 for pipe damage. For free-spanning damage, the severities are valued from 0.0 to 0.9 in numerical simulations. Therefore, for this kind of damage, $m_3$=10 if the increment is taken as 0.1. Totally, there are 240 damage cases. Numerical simulations are performed for these cases as well as the intact structure case.

**Damage identification under noise free condition**

This section focuses on damage identification under noise free condition. The simulated data with an assumed pipe damage ($L_p = 3; \theta_p = 0.86$) and free-spanning damage ($L_s = 11; \theta_s = 0.82$) are used in damage identification analysis. As described above, the multi-step approach used to identify multiple damages is adopted here to identify multiple types of damage. In the analysis, the pipe damage is identified first, followed by the free-spanning damage.

The identification results are summarized in Table 4. To demonstrate the independence of the method on random generations of matrices as described in subsection of damage identification scheme, the identification analyses are performed for three times, indicated as No. 1, 2 and 3 with three sets of independently generated random matrices. As shown in Table 4, irrespective of the random matrices, in Step 1, the damage types can be easily identified by using the proposed method for both damage cases. In Step 2, the right damage locations are also correctly identified for both types of damage. In Step 3, the damage severities are also approximately identified, and the identification results are almost independent of the randomly generated matrices. These results demonstrate the accuracy and efficiency of the proposed method in identifying multiple types of damages using noise free data measured at a single location.

**Damage identification under different noise levels**

In order to further demonstrate the effectiveness of the proposed method in practical applications, it is used for damage identification under different noise levels. The same two simulated damage cases

are selected, specifically, $(L_p = 3; \theta_p = 0.86)$ and $(L_s = 11; \theta_s = 0.82)$. Three noise levels are considered, namely 1%, 5% and 10%. The results are given in Table 5. As shown, under different noise levels, the pipeline damage is successfully identified even under 10% noise. The free-spanning damage location is also correctly identified under the three assumed noise levels, but the damage severity is only correctly identified when the noise level is 1%. When the noise level is 5% or more, the free-spanning damage severity is significantly overestimated. The reason is that the influence of free-spanning stiffness in such a small area on pipeline vibration is insignificant since pipe itself is stiffer than soil. The effect of reducing the soil stiffness by 18% in a short span on pipe vibrations is overshadowed by the influences of noise. Nonetheless, the results demonstrate that the proposed algorithm is robust even under high noise levels in identifying structural damages by using only a single measurement.

# Experimental verifications

## *Experimental setup and test results*

To further verify the reliability of the proposed method, a scaled pipeline model was designed and tested in the laboratory. It is a 6.5 m long steel pipe. Two concrete blocks, weighing 19 kg respectively, were placed 100 mm from each end of the pipeline. The pipe was partially filled with water. The model is shown in Figure 2. The geometrical and material properties of the pipe and soil are summarized in Table 1. It should be noted that the soil under the pipeline was manually compacted before the pipe was laid. Once the pipeline model was placed on the ground, the pipe was half buried into the soil. Again, the soil was manually compacted and left to settle for a few months before the experimental testing was carried out.

The impact hammer tests were carried out with Dytran 5802A impact hammer and 15 KISTLER 8330 accelerometers. Fifteen measuring points, showed in Figure 3, were evenly distributed along the pipe. The impact point is located at $0.19L$ of the pipe to avoid a node of the interesting modes. The sampling rate is 2000 Hz. 20480 points are recorded for each channel.

The intact pipe-soil system was tested first. Then, the soil under the third segment was removed, which is used to simulate the system with complete (100%) spring damage $(L_s = 4; \theta_s = 0)$. It should be noted that in the test, it is difficult to control the foundation spring stiffness, therefore only the complete removal of the soil underneath the certain pipe segment to simulate free-spanning damage is carried out. For both the undamaged and damaged cases, the test is repeated 6 times and the averaged records are used in the analysis to minimize the noise/error effects. More detailed

results on modal parameters can be found in Wang et al. (2010). It should be noted that the information of all the 15 sensors need be used to get the modal parameters, while the method proposed in this study only requires the signals measured at one accelerometer. The comparison of the acceleration time histories on accelerometer 2 with and without free-spanning damage is shown in Figure 4, which do not show apparent differences under two circumstances.

## *Damage identification by using the proposed method*

In this section, the recorded acceleration time histories with and without free-spanning damage are used for experimental verification of the proposed method. The similar training data based on pipe-soil system with different damage scenarios are used in damage identification. In order to regulate the data, the tested data are reshaped into 1000 Hz; the duration is taken as 1 second; and the amplitude is scaled to the same level as the training data. Although intuitively the time histories of the experimental results and numerical results used to train the model are different, the proposed method still correctly identifies the damage type in Step 1. In Step 2, the exact damage location can be identified. In Step 3, the spring damage is quantified as 0.2, which is close to the real damage parameter of 0 after completely removing the soil beneath the pipe. It should be noted that improved identification results, i.e., the damage severity, can be obtained by using more refined numerical models and more training data. However, even by using limited training data based on the simplified FE model, the proposed damage identification scheme is capable of identifying the damage location exactly and severity approximately by using only a single measurement, demonstrating the superiority of the method for application in structural health monitoring.

## *Discussions*

It is worth noting that the formulated problem (Eq. (8)) can be classified into three categories, $m = n$, $m < n$ or $m > n$. When $m = n$, the solution is unique if A is of full rank matrix. If it is over-determined ($m > n$), the problem is traditionally solved through Eq. (9), as a standard least squares problem. Unfortunately, in the presence of data noise (which is unavoidable in civil engineering practices), such solution may not be perfectly found (Wright et al. 2009). As for under-determined case ($m < n$), theoretically there would be many solutions and we need to find the sparsest solution for pattern recognition purposes. In this paper, the general cases are considered, where a solution should work on all the above cases. Therefore, the damage identification problem is finally formulated as Eq. (10), by introducing a random matrix to the linear system (Eq. (8)). The benefits are two-folded. First, the linear system in Eq. (8) is usually high-dimensional. The direct solution is computationally inefficient and may beyond the capability of regular computers (Wright et al. 2009).

501 The introduction of random matrices can effectively reduce data dimension and computational cost.
502 Second, the robustness of the algorithm can be achieved. CS is well-known for its stable signal
503 recovery capability with incomplete and inaccurate measurements (Candes et al., 2006b). By
504 introducing random matrices which satisfy RIP and incoherence conditions, the identification via $l_1$
505 optimization becomes robust.

506 In this study, numerically simulated training data are used for structural damage identifications
507 based on numerical simulated (Section of numerical studies) and experimental measured data
508 (Section of experimental verifications). The results demonstrate that the proposed method is robust
509 to the modeling errors and measurement noises. Although only a simple pipe-soil model is used in
510 this study to demonstrate the efficiency of the method, it can be used to identify conditions of
511 complex structures. The challenge of applying the method to complex large-scale civil structures is
512 the time needed to perform numerical simulation of the damage cases for training the model. In fact,
513 it may be not practical to build a high-quality numerical model and then to conduct parametric
514 studies for all the possible damage patterns for a large civil structure. In these cases, sub-structuring
515 method might be adopted. A numerical model with only substructures should be built to define the
516 damage patterns, i.e., the damage type, location and severity to identify damages in the substructure.
517 This procedure can be applied progressively to cover all the structural parts with possible damages.
518 However, application of this approach to identify damages in a large structure is out of the scope of
519 the present paper and may be explored in the future.

520 It should be also noted that the structural responses of only one sensor (sensor 2) are used for
521 damage identification in this study. Theoretically, the data from other sensors should yield similar
522 identification results, while the data from more sensors will yield even better results. However, these
523 will require more training data. More parametric studies should be done as shown in subsection of
524 numerical model. These works will be done in the future.

# 525 Conclusions

526 This paper proposes a new damage identification scheme based on sparse representation of time
527 domain structural responses and CS techniques. After briefly introducing CS theory, the structural
528 damage identification problem is shaped into sparse representation based pattern classification
529 problem. To solve this problem, a feature matrix is first constructed based on the sparse
530 representation results of time domain structural responses. Then, a three-step damage classification
531 algorithm by using $l_1$-MAGIC is proposed. The effectiveness of the proposed method is
532 demonstrated by both numerical and experimental examples. Based on the results, the following

conclusions can be drawn:

1. Demonstrated by both numerical and experimental verification results, the proposed CS based damage identification scheme is robust. It can identify multiple types of damages, damage locations and severities even under high noise levels with minimum numbers of vibration measurements. Therefore, it is suitable for online damage identification of civil infrastructure.
2. Compared with traditional methods, the proposed scheme requires less information, i.e., vibration time history of one point on the structure can yield good identification results.
3. The proposed damage identification scheme has shown great application potential. Case studies of practical structures will be performed in the near future.

# Acknowledgements

This work is partially supported by the Collaborative Research Center for Integrated Engineering Asset Management (CIEAM II).

We also thank the authors of $l_1$-magic for their generous online distribution.

# References

Adeli, H. and Jiang, X. (2006). "Dynamic fuzzy wavelet neural network model for structural system identification." *Journal of Structural Engineering-ASCE*, Vol.132, No.1, pp. 102-111.

Bakhary N., Hao H. and Deeks A.J. (2007). "Damage detection using artificial neural network with consideration of uncertainties." *Engineering Structure*, 29(11), 2806-2815.

Bao Y.Q., Beck J.L. and Li H. (2010) "Compressive sampling for accelerometer signals in structural health monitoring." *Structural Health Monitoring*, DOI: 10.1177/1475921710373287

Baraniuk R.G. (2007) "Compressive sensing." Lecture Notes in *IEEE Signal Processing Magazine*, vol. 24, no. 4, pp. 118-120

Borgnat P. and Flandrin P. (2008) "Time- frequency localization from spasity constraints." *IEEE International Conference on Acoustic, Speech, and Signal Processing (ICASSP)*, Las Vegas, USA

Candes E.J. (2006) "Compressive sampling." *Proceedings of the International Congress of Mathematicians*, Madrid, Spain.

560 Candes E.J., Romberg J.K. (2005) "$l_1$-MAGIC: recovery of Sparse Signals via convex
561 programming." Matlab Program, http://www.acm.caltech.edu/l1magic/

562 Candes E.J., Romberg J.K. and Tao T. (2006a) "Robust uncertainty principles: Exact signal
563 reconstruction from highly incomplete frequency information." *IEEE Transactions On Information*
564 *Theory*, vol. 52, pp. 489-509

565 Candes E.J., Romberg J.K. and Tao T. (2006b) "Stable Signal Recovery from Incomplete and
566 Inaccurate Measurements." *Communications on Pure and Applied Mathematics*, vol. 59, no. 8, pp.
567 1207-1223

568 Candes E.J. and Tao T. (2005) "Decoding by linear programming." *IEEE Transactions on*
569 *Information Theory*, vol. 51, no. 12, pp. 4203-4215

570 Chen B. and Zang C.Z. (2009) "Artificial immune pattern recognition for structure damage
571 classification." *Computers and Structures*, vol. 87, 1394-1407

572 Chen S.S. , Donoho D.L. and Saunders M.A. (2001) "Atomic decomposition by basis pursuit."
573 *SIAM Review*, Society for Industrial and Applied Mathematics, 43(1), 129-159

574 Cortial J., Farhat C., Guibas L.J. and Rajashekhar M. (2007) "Compressed sensing and time-parallel
575 reduced-order modeling for structural health monitoring using a DDDAS." *Lecture Notes in*
576 *Computer Science*, vol. 4487, 1171-1179

577 Donoho D.L. (2006) "Compressed sensing." *IEEE Transactions On Information Theory*, vol. 52, pp.
578 1289-1306.

579 Donoho D.L. and Huo X. (2001) "Uncertainty principles and ideal atomic decomposition." *IEEE*
580 *Transactions on Information Theory*, vol. 47, 2845-2862

581 Duarte M.F., Davenport M.A., Takhar D., Laska J.N., Sun T., Kelly K.F. and Baraniuk R.G. (2008)
582 "Single-pixel imaging via compressive sampling." *IEEE Signal Processing Magazine*, vol. 25, no. 2,
583 pp. 83-91

584 Eldar Y.C. and Kutyiok G. (2012) *Compressed sensing*. Cambridge University Press

585 Gurbuz A.C., McClellan J.H. and Scott W.R. (2009) "A compressive sensing data acquisition and
586 imaging method for stepped frequency GPRs." *IEEE Transactions on Signal Processing*, 57(7),

587 2640-2650

588 Gul M. and Catbas F.N. (2009) “Statistical pattern recognition for structural health monitoring using
589 time series modeling: theory and experimental verifications.” *Mechanical Systems and Signal*
590 *Processing*, vol. 23, 2192-2204

591 Hao H. and Xia Y. (2002) “Vibration-based damage detection of structures by genetic algorithm.”
592 *Journal of Computing in Civil Engineering ASCE*, 16(3), 222-229.

593 Kim H. and Melhem H. (2004) “Damage detection of structures by wavelet analysis.” *Engineering*
594 *Structures*, 26, 347-362

595 Kolakowski P., Mujica L.E. and Vehi J. (2006) “Two approaches to structural damage identification:
596 model updating versus soft computing.” *Journal of Intelligent Material Systems and Structures*, 17,
597 63-79

598 Lu W. and Vaswani N. (2009) “Modified compressive sensing for real-time dynamic MR imaging.”
599 *IEEE International Conference On Image Processing*, Cairo, Egypt

600 Rytter A. (1993) *Vibration Based Inspection of Civil Engineering Structures* [PhD Thesis] Aalborg
601 University, Denmark.

602 Sohn H. Farrar C.R., Hunter N.F. and Worden K. (2001) “Structural health monitoring using
603 statistical pattern recognition techniques.” *Journal of Dynamic Systems, Measurement, and Control-*
604 *ASME*, vol. 123, 706-711

605 Sohn H., Farrar C.R., Hemez F.M., Czarnecki J.J., Shunk D.D., Stinemates D.W., Nadler B.R.
606 (2003) “A review of structural health monitoring literature: 1996-2001.” *Los Alamos National*
607 *Laboratory Report*; LA-13976-MS.

608 Taha M.M.R. and Lucero J. (2005) “Damage identification for structural health monitoring using
609 fuzzy pattern recognition.” *Engineering Structures*, 27, 1774-1783

610 Wakin M.B., Laska J.N., Duarte M.F., Baron D., Savotham S., Takhar D., Kelly K.F. and Baraniuk
611 R.G. (2006) “An architecture for compressive imaging.” *IEEE International Conference on Image*
612 *Processing*, Atlanta, USA

613 Wang Y. and Hao H. (2010) “An introduction to compressive sensing and its potential applications

614 in structural engineering." *The 11th International Symposium on Structural Engineering*, Guangzhou,
615 China

616 Wang Y., Hao H. and Peng X.L. (2010) "Simplified pipeline-soil interaction model for vibration-
617 based damage detection of onshore pipelines." *ISSE11: The 11th International Symposium on*
618 *Structural Engineering*, Guangzhou, China.

619 Wright J., Yang A.Y., Ganesh A., Sastry S.S. and Ma Y. (2009) "Robust face recognition via sparse
620 representation." *IEEE transactions on Pattern Analysis and Machine Intelligence*, 31(2), 210-227

621 Yang A.Y., Wright J., Ma Y. and Sastry S.S. (2007) "Feature selection in face recognition: a sparse
622 representation perspective." *Technical report in University of California, Berkeley,* No. UCB/EECS-
623 2007-99

624 Yang J.N., Lei Y., Lin S. and Huang N. (2004) "Hilbert-Huang based approach for structural damage
625 detection." *Journal of Engineering Mechanics ASCE*, 130(1), 85-95

626

627 # Notation

| | |
|---|---|
| $\mathbf{A}$ | The feature matrix |
| $\widetilde{\mathbf{A}}$ | Rearranged feature matrix |
| $D_i$ | Inner diameter of the pipe |
| $D_o$ | Outer diameter of the pipe |
| $E$ | Young's Modulus of the pipe |
| $E(r_j)$ | The average difference between feature of new signal and $\delta_j(\mathbf{z})$ |
| $\mathbf{f}$ | Signal vector |
| $i$ | Counting number from 1 to $N$ |
| $j$ | The $j^{\text{th}}$ Damage pattern |
| $K$ | Number of (sparse) basis vectors |
| $k$ | Counting number from 1 to $M$ |
| $K_s$ | Stiffness of soil (per element 0.0742m) |
| $K_r$ | Rotational stiffness of two concrete blocks |
| $L$ | Total length of beam |
| $l$ | Counting number from 1 to $n_j$ |
| $L_n$ | Length of the pipe |
| $L_p$ | Pipe damage location |
| $L_s$ | Soil support damage location |
| $M$ | Dimension of measurement vector |
| $m$ | Number of damage patterns |
| $m_1$ | Number of damage types |
| $m_2$ | Number of damage locations |
| $m_3$ | Number of damage severities |
| $N$ | Dimension of signal vector |
| $n$ | Total number of signals/features |
| $n_j$ | Number of signals associated with damage pattern $j$ |
| $p$ | Counting number from 1 to $q$ |
| $q$ | Number of random projection matrices |
| $r_j^p(\mathbf{z})$ | The residual between feature of new signal and $\delta_j(\mathbf{z})$ using $p^{\text{th}}$ random matrix, as shown in Eq. (12) |
| $t$ | Thickness of the pipe |

| | |
|---|---|
| $\mathbf{v}_{j,l}$ | The $l^{\text{th}}$ feature of the training data associated with damage pattern $j$ |
| $\tilde{\mathbf{v}}$ | Rearranged feature vector for new signal |
| $\mathbf{x}$ | Weighting coefficients |
| $\mathbf{y}$ | Measurement vector |
| $\mathbf{z}$ | The coefficient vector whose entries are mostly zero except those associated with damage pattern $j$ |
| $\alpha_{j,l}$ | Sparse representation scalars |
| $\delta_j(\mathbf{z})$ | The vector whose only nonzero entries are the entries in $\mathbf{z}$ that are associated with damage $j$, and whose entries associated with all other subjects are zero. |
| $\varepsilon$ | Error tolerance for $l_1$ optimization |
| $\rho$ | Density of the pipe |
| $\rho_w$ | Water density (equal to steel area) |
| $\Phi$ | Projection matrix |
| $\Theta$ | An $M \times N$ matrix |
| $\theta_p$ | Pipe damage severity |
| $\theta_s$ | Soil support damage severity |
| $\mu$ | Coherence measurement |
| $\Psi$ | Decomposition basis |

628

# Tables

Table 1. Pipeline Properties (data from Wang et al., 2010)

| Parameters | Description | Value | Units |
|---|---|---|---|
| $L_n$ | Span length | 5936 | *mm* |
| $D_o$ | Outer diameter of the pipe | 48.3 | *mm* |
| $D_i$ | Inner diameter of the pipe | 41.9 | *mm* |
| $t$ | Thickness of the pipe | 3.2 | *mm* |
| $E$ | Young's Modulus of the pipe material | 200 | *GPa* |
| $\rho$ | Density of the pipe material | 7850 | $kg/m^3$ |
| $\rho_w$ | Water density (equal to steel area) | 2630 | $kg/m^3$ |
| $K_s$ | Stiffness of soil (per element 0.0742m) | 7035 | *N/m* |
| $K_r$ | Rotational stiffness of two concrete blocks | $8.189 \times 10^4$ | *Nm/rad* |

633 Table 2. Summary of damage identification results under noise-free condition

| Case | No. | Option 1 | Option 2 |
|---|---|---|---|
| $L_p = 13; \theta = 0.56$ | 1 | $L_p = 13;\ \theta = 0.6$ | $L_p = 13;\ \theta = 0.8$ |
| | 2 | $L_p = 13;\ \theta = 0.6$ | $L_p = 13;\ \theta = 0.9$ |
| | 3 | $L_p = 13;\ \theta = 0.6$ | $L_p = 13;\ \theta = 0.6$ |
| $L_p = 4; \theta = 0.82$ | 1 | $L_p = 4;\ \theta = 0.8$ | $L_p = 4;\ \theta = 0.8$ |
| | 2 | $L_p = 4;\ \theta = 0.8$ | $L_p = 4;\ \theta = 0.7$ |
| | 3 | $L_p = 4;\ \theta = 0.8$ | $L_p = 4;\ \theta = 0.9$ |

634

635

636 Table 3. Summary of damage identification results under different noise levels

| Case | No. | 1% noise | 5% noise | 10% noise |
|---|---|---|---|---|
| $L_p = 13;$ | 1 | $L_p = 13;\ \theta = 0.6$ | $L_p = 13;\ \theta = 0.6$ | $L_p = 13; \theta = 0.6$ |
| | 2 | $L_p = 13; \theta = 0.6$ | $L_p = 13;\ \theta = 0.6$ | $L_p = 13; \theta = 0.6$ |
| $\theta = 0.56$ | 3 | $L_p = 13;\ \theta = 0.6$ | $L_p = 13;\ \theta = 0.6$ | $L_p = 13; \theta = 0.6$ |
| $L_p = 4;$ | 1 | $L_p = 4;\ \theta = 0.8$ | $L_p = 4;\ \theta = 0.8$ | $L_p = 4;\ \theta = 0.8$ |
| | 2 | $L_p = 4;\ \theta = 0.8$ | $L_p = 4;\ \theta = 0.8$ | $L_p = 4;\ \theta = 0.8$ |
| $\theta = 0.82$ | 3 | $L_p = 4;\ \theta = 0.8$ | $L_p = 4;\ \theta = 0.8$ | $L_p = 4;\ \theta = 0.8$ |

637

638

639 Table 4. Summary of damage identification results with multiple types of damages

| Case | No. | Step 1: Damage type | Step 2: Damage location | Step 3: Damage severity |
|---|---|---|---|---|
| $L_p = 3; \theta_p = 0.86$ | 1 | Pipe | $L_p = 3$ | $\theta_p = 0.9$ |
| | 2 | Pipe | $L_p = 3$ | $\theta_p = 0.9$ |
| | 3 | Pipe | $L_p = 3$ | $\theta_p = 0.9$ |
| $L_s = 11;\ \theta_s = 0.82$ | 1 | Spring | $L_s = 11$ | $\theta_s = 0.8$ |
| | 2 | Spring | $L_s = 11$ | $\theta_s = 0.9$ |
| | 3 | Spring | $L_s = 11$ | $\theta_s = 0.8$ |

640

641

642 Table 5. Summary of damage identification results with multiple types of damages
643 under different noise levels

| Case | Noise level | Step 1: Damage type | Step 2: Damage location | Step 3: Damage severity |
|---|---|---|---|---|
| $L_p = 3; \theta_p = 0.86$ | 1% | pipe | $L_p = 3$ | $\theta_p = 0.9$ |
| | 5% | pipe | $L_p = 3$ | $\theta_p = 0.9$ |
| | 10% | pipe | $L_p = 3$ | $\theta_p = 0.9$ |
| $L_s = 11;\ \theta_s = 0.82$ | 1% | spring | $L_s = 11$ | $\theta_s = 0.9$ |
| | 5% | spring | $L_s = 11$ | $\theta_s = 0.5$ |
| | 10% | spring | $L_s = 11$ | $\theta_s = 0.4$ |

644

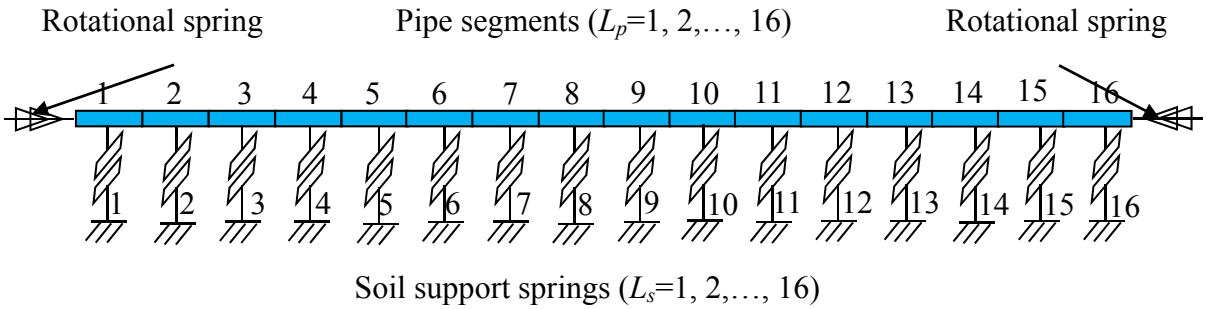


Figure 1. Simplified pipe-soil interaction finite element model

Figure 2. Pipeline test model

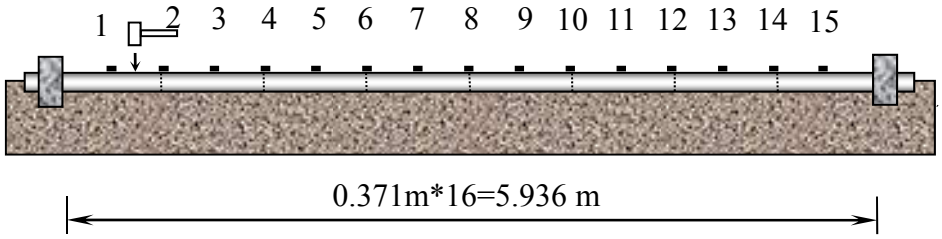


Figure 3. Locations of measurement points

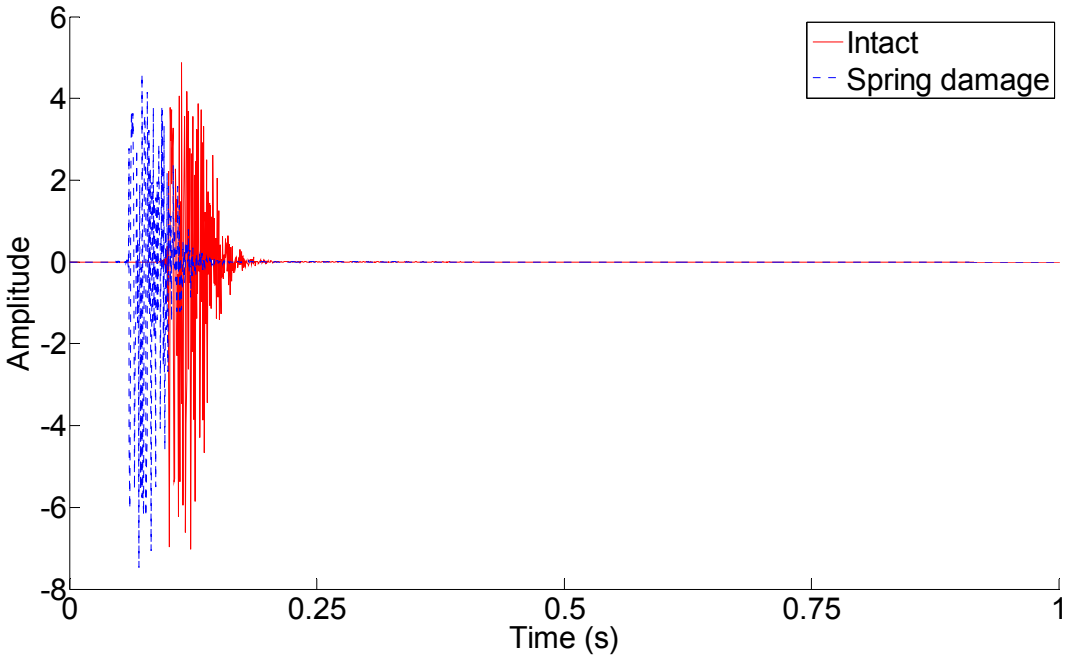


a) Overview

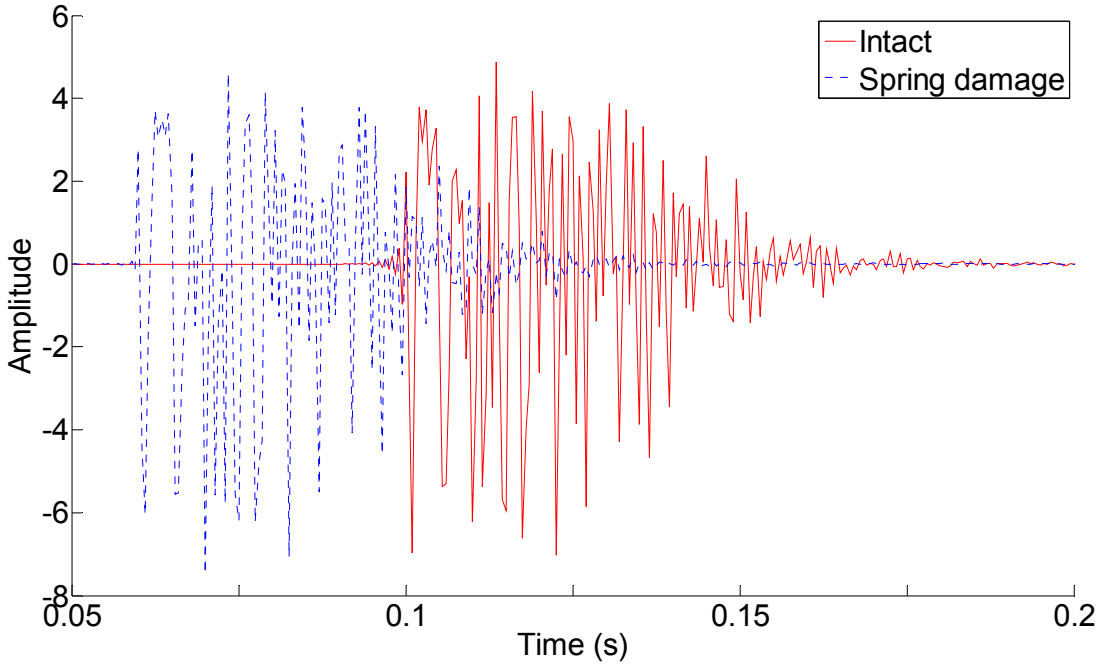


b) Detailed plot

Figure 4. Acceleration time histories of sensor 2